Study on the rare radiative decay $B_c \to D_s^* \gamma$ in the standard model and multiscale walking technicolor model

Gongru Lu[a,b], Chongxing Yue[a,b], Yigang Cao[a], Zhaohua Xiong[a], Zhenjun Xiao[a,b]

a. Physics Department of Henan Normal University, Xinxiang, Henan, 453002, P. R. China*

b. CCAST (world laboratory), P.O.Box 8732, Beijing, 100080, P. R. China

Abstract

Applying the perturbative QCD (PQCD) method, we study the decay $B_c \to D_s^* \gamma$ in the standard model and multiscale walking technicolor model. In the SM, we find that the contribution of weak annihilation is more important than that of the electromagnetic penguin. The presence of Pseudo-Goldstone-Bosons (PGBs) in MWTCM leads to a large enhancement in the rate of $B_c \to D_s^* \gamma$, but this model is in conflict with the branching ratio of $Z \to b\overline{b}$ (R_b) and the CLEO data on the branching ratio BR ($b \to s\gamma$). If topcolor is further introduced, the calculated results in the topcolor assisted MWTCM can be suppressed and be in agreement with the CLEO data for a certain range of the parameters.

PACS numbers: 12.15.LK, 12.60.Nz, 13.30.Eg

* mailing address

1. Introduction

The inclusive rare decay $B \to X_s \gamma$ has been studied several years ago [1]. Recently the physics of B_c meson has caught intensive attentions[2]. The B_c meson is believed to

be the next and the final family of B mesons, it provides unique opportunity to examine various heavy quark fragmentation models, heavy quark spin-flavor symmetry, different quarkonium bound state models and properties of inclusive decay channels. Furthermore, the radiative weak decays of B_c meson also offer a rich source to measure CKM matrix elements of the standard model (SM). In this paper, we will address B_c radiative decay $B_c \to D_s^* \gamma$.

Different from the decay $B \to X_s \gamma$ which is mainly induced by the flavor-changing $b \to s\gamma$ neutral currents [3], the bound state effects in the decay $B_c \to D_s^* \gamma$ may be rather large. Bound state effects include modifications from weak annihilation which involve no neutral flavor-changing currents at all. The effects of weak annihilation mechanism are expected rather large due to the large CKM amplitude. We will address this point in detail below.

Unfortunately, the well-known chiral-symmetry [4] and the heavy quark symmetry [5] can not be applied to this process. Recently, a perturbative QCD (PQCD) analysis of B meson decays seems give a good prediction [6]. As it is argued in Ref.[7] that two body nonleptonic decay of B_c meson can be conveniently studied within the framework of PQCD suggested by Brodsky-Lepage [8] and then developed in Ref.[6]. Here, we preview the reliability of PQCD analysis of B_c radiative decay: in the process $b \to s\gamma$, s quark obtains large momentum by recoiling, in order to form a bound state with the spectator $\overline{c}$ quark, the most momentum of s quark must be transferred to $\overline{c}$ by a hard scattering process. PQCD [6, 8] can be used in the calculation for the hard scattering process because the heavy charm usually share the most momentum of final state (i.e. D_s^*). The relevant Feynman diagrams are given in Fig.1.

Like in $B \to K^* \gamma$, the subprocess $b \to s\gamma$ in $B_c \to D_s^* \gamma$, is usually controlled by the one-loop electromagnetic penguin diagrams (Fig.1.a). It plays an important role in testing loop effects in the SM and in searching for the physics beyond the SM (so called new physics).

Most recently, the contribution of the electromagnetic penguin interaction to the branching ratio BR ($b \to s\gamma$) from PGBs in the one generation technicolor model (OGTM) has been estimated in Ref.[9]. However, we know that there are some problems (such as flavor-changing neutral currents (FCNCs), the large positive contributions to the parameters) in most conventional TC models. Walking technicolor (WTC) has

been advocated as a solution to the problem of large flavor-changing neutral current interactions in extended technicolor (ETC) theories of quark and lepton mass generation [10]. Furthermore, the electroweak parameter S in WTC models is smaller than that in the simple QCD-like ETC models and consequently its deviation from the SM value may fall within current experimental bounds [11]. To explain the large hierarchy of the quark masses, multiscale WTC models (MWTCM) are further proposed [12].

However, as discussed in Ref.[13], the correction of PGBs in MWTCM to the $Z \to b\overline{b}$ branching ratio (R_b) is too large when compared with recent LEP data. In this paper we calculated the contribution to the branching ratio $B_c \to D_s^* \gamma$ from the PGBs in MWTCM and found that such contribution is too large when compared with CLEO constraint for the inclusive decay $b \to s\gamma$. In general, there are two mechanisms which contribute to the decay $B_c \to D_s^* \gamma$: one proceeds through the short distance $b \to s\gamma$ transition while the other through weak annihilation accompanied by a photon emission. On the other hand, if topcolor [14] is further introduced to the multiscale walking technicolor model, the modification from the PGBs in the topcolor assisted multiscale walking technicolor model (TAMWTCM) to $B_c \to D_s^* \gamma$ is strongly suppressed, and therefore can be consistent with the recent CLEO data for the branching ratio BR ($b \to s\gamma$) [15].

This paper is organized as follows: In Sec.2, we display our calculations in the SM and MWTCM. We present the final numerical results in Sec.3. Sec.4 contains the discussion.

2. Calculation

Using the factorization scheme [8] within PQCD, the momentum of quarks are taken as some fractions x of the total momentum of the meson weighted by a soft physics distribution functions $\Phi_H(x)$. The peaking approximation is used for $\Phi_H(x)$ [16], the distributition amplitude of B_c and D_s^* are

$$\Phi_{B_c}(x) = \frac{f_{B_c}\delta(x - \epsilon_{B_c})}{2\sqrt{3}}, \tag{1.a}$$

$$\Phi_{D_s^*}(x) = \frac{f_{D_s^*}\delta(x - \epsilon_{D_s^*})}{2\sqrt{3}}, \tag{1.b}$$

where f_{B_c}, $f_{D_s^*}$ are decay constants of B_c and D_s^* respectively, and

$$\epsilon_{B_c} = \frac{m_c}{m_{B_c}}, \tag{1.c}$$

$$\epsilon_{D_s^*} = \frac{m_{D_s^*} - m_c}{m_{D_s^*}}. \tag{1.d}$$

The spinor parts of B_c and D_s^* wave functions are

$$\frac{(\not{p} + m_{B_c})\gamma_5}{\sqrt{2}}, \tag{2.a}$$

$$\frac{(\not{p} - m_{D_s^*})\ \not{\epsilon}}{\sqrt{2}}, \tag{2.b}$$

where ϵ is the polarization vector of D_s^*.

2.1. Electromagnetic penguin contribution

The short distance electromagnetic penguin process is governed by the electromagnetic penguin operators [1]. At the weak scale $\mu = m_b$, the effective Hamiltonian for $b \to s\gamma$ transition is

$$H_{eff} = \frac{4G_F}{\sqrt{2}} V_{tb} V_{ts}^* C_7(m_b) O_7, \tag{3}$$

where

$$O_7 = \frac{e m_b \overline{s} \sigma_{\mu\nu} F^{\mu\nu} (1+\gamma_5) b}{32\pi^2} \tag{4.a}$$

and which is denoted by a blob in Fig.1.a. The corresponding coefficient of O_7 has the form

$$C_7(m_b) = \varrho^{-\frac{16}{23}} [C_7(m_W) + \frac{8}{3}(\varrho^{\frac{2}{23}} - 1) C_8(m_W)] + C_2(m_W) \sum_{i=1}^{8} h_i \varrho^{-a_i} \tag{4.b}$$

with

$$\varrho = \frac{\alpha_s(m_b)}{\alpha_s(m_W)}, \quad C_2(m_W) = -1, \tag{4.c}$$

$$h_i = (\frac{626126}{272277}, -\frac{56281}{51730}, -\frac{3}{7}, -\frac{1}{14}, -0.6494, -0.0380, -0.0186, -0.0057),$$

$$a_i = (\frac{14}{23}, \frac{16}{23}, \frac{6}{23}, -\frac{12}{23}, 0.4086, -0.4230, -0.8994, 0.1456). \tag{4.d}$$

And $C_7(m_W) = \frac{1}{2}A(x)$, $C_8(m_W) = \frac{1}{2}C(x)$ in the standard model with $x = (\frac{m_t}{m_W})^2$. The functions $A(x)$ and $C(x)$ arise from graphs with W boson exchange.

In MWTCM, the relevant Feynman rules are the same as Ref.[17]:

$$[p^+ - u_i - d_j] = i\frac{1}{\sqrt{6}F_Q} V_{u_i d_j} [m_{u_i}(1-\gamma_5) - m_{d_j}(1+\gamma_5)], \tag{5.a}$$

$$[p_8^+ - u_i - d_j] = i\frac{V_{u_i d_j}}{F_Q} \lambda^a [m_{u_i}(1-\gamma_5) - m_{d_j}(1+\gamma_5)], \tag{5.b}$$

where $u=(u,c,t)$, $d=(d,s,b)$ and $V_{u_id_j}$ is the element of CKM matrix, and finally F_Q is the decay constant of technipions composed of Q in MWTCM.

By explicit calculations, one can get [9]

$$C_7(m_W)=\frac{1}{2}A(x)+\frac{1}{3\sqrt{2}G_FF_Q^2}[B(y)+8B(z)], \tag{5.c}$$

$$C_8(m_W)=\frac{1}{2}C(x)+\frac{1}{3\sqrt{2}G_FF_Q^2}[D(y)+(8D(z)+E(z))], \tag{5.d}$$

where $y=(\frac{m_t}{m_{p^\pm}})^2$, $z=(\frac{m_t}{m_{p_8^\pm}})^2$. The functions B, D and E arise from diagrams with color singlet and color octet charged PGBs of MWTCM, and the explicit expressions for relevant functions are as follows:

$$A(x)=-\frac{x}{12(1-x)^4}[(1-x)(8x^2+5x-7)+6x(3x-2)\ln x], \tag{6.a}$$

$$B(x)=\frac{x}{72(1-x)^4}[(1-x)(22x^2-53x+25)+6(3x^2-8x+4)\ln x], \tag{6.b}$$

$$C(x)=-\frac{x}{4(1-x)^4}[(1-x)(x^2-5x-2)-6x\ln x], \tag{6.c}$$

$$D(x)=\frac{x}{24(1-x)^4}[(1-x)(5x^2-19x+20)-6(x-2)\ln x], \tag{6.d}$$

$$E(x)=-\frac{x}{8(1-x)^4}[(1-x)(12x^2-15x-5)+18x(x-2)\ln x]. \tag{6.e}$$

Now we write down the amplitude of Fig1.a as

$$\begin{aligned} M_a= \ & \int_0^1 dx_1dy_1\Phi_{D_s^*}(y_1)\Phi_{B_c}(x_1)\tfrac{-iG_F}{\sqrt{2}}V_{tb}V_{ts}^*C_7(m_b)m_be\tfrac{\alpha_s(m_b)}{2\pi}C_F \\ & \{T_r[(\not{q}-m_{D_s}^*)\ \not{\epsilon}\sigma_{\mu\nu}(1+\gamma_5)k^\nu\eta^\mu(\not{p}-y_1\ \not{q}+m_b)\gamma_\alpha(\not{p}+m_{B_c})\gamma_5\gamma^\alpha]\tfrac{1}{D_1D_3} \\ & +Tr[(\not{q}-m_{D_s^*})\ \not{\epsilon}\gamma_\alpha(\not{q}-x_1\ \not{p})\sigma_{\mu\nu}(1+\gamma_5)k^\nu\eta^\mu(\not{p}+m_{B_c})\gamma_5\gamma^\alpha]\tfrac{1}{D_2D_3}\}, \end{aligned} \tag{7}$$

where η is the polarization vector of photon, x_1, y_1 are the momentum fractions shared by charms in B_c and D_s^*, respectively. The functions D_1, D_2 and D_3 in equation (7) are the forms of

$$D_1=(1-y_1)(m_{B_c}^2-m_{D_s^*}^2y_1)-m_b^2, \tag{8.a}$$

$$D_2=(1-x_1)(m_{D_s^*}^2-m_{B_c}^2x_1), \tag{8.b}$$

$$D_3=(x_1-y_1)(x_1m_{B_c}^2-y_1m_{D_s^*}^2). \tag{8.c}$$

After explicit calculation, the amplitude M_a can be written as the form of

$$M_a=i\varepsilon_{\mu\nu\alpha\beta}\eta_\mu k^\nu\epsilon^\alpha p^\beta f_1^{peng}+\eta^\mu[\epsilon_\mu(m_{B_c}^2-m_{D_s}^2)-(p+q)_\mu(\epsilon\cdot k)]f_2^{peng} \tag{9}$$

with form factors

$$f_1^{peng} = 2f_2^{peng} = C\int_0^1 dx_1 dy_1 \delta(x_1-\epsilon_{B_c})\delta(y_1-\epsilon_{D_s^*}) \cdot\{[m_{B_c}(1-y_1)(m_{B_c}-2m_{D_s^*})-m_b(2m_{B_c}-m_{D_s^*})]\frac{1}{D_1D_3} - m_{B_c}m_{D_s^*}(1-x_1)\frac{1}{D_2D_3}\}, \quad (10.a)$$

where

$$C = \frac{em_b f_{B_c} f_{D_s^*} C_7(m_b) C_F \alpha_s(m_b) G_F V_{tb} V_{ts}^*}{12\pi\sqrt{2}}. \quad (10.b)$$

2.2. The weak annihilation contribution

As mentioned in Sec.1, B_c meson is also the unique probe of the weak annihilation mechanism.

In SM, using the formalism developed by H. Y. Cheng *et al.* [18], the amplitude of annihilation diagrams (see Fig.1.b) is

$$M_b^{(W)} = i\varepsilon_{\mu\nu\alpha\beta}\eta^\mu k^\nu \epsilon^\alpha p^\beta f_{1(W)}^{anni} + \eta^\mu[\epsilon_\mu(m_{B_c}^2 - m_{D_s}^2) - (p+q)_\mu(\epsilon\cdot k)]f_{2(W)}^{anni} \quad (11)$$

with

$$f_{1(W)}^{anni} = 2\zeta[(\frac{e_s}{m_s}+\frac{e_c}{m_c})\frac{m_{D_s^*}}{m_{B_c}} + (\frac{e_c}{m_c}+\frac{e_b}{m_b})]\frac{m_{D_s^*}m_{B_c}}{m_{B_c}^2 - m_{D_s^*}^2}, \quad (12.a)$$

$$f_{2(W)}^{anni} = -\zeta[(\frac{e_s}{m_s}-\frac{e_c}{m_c})\frac{m_{D_s^*}}{m_{B_c}} + (\frac{e_c}{m_c}-\frac{e_b}{m_b})]\frac{m_{D_s^*}m_{B_c}}{m_{B_c}^2 - m_{D_s^*}^2}, \quad (12.b)$$

where

$$\zeta = ea_2\frac{G_F}{\sqrt{2}}V_{cb}V_{cs}^* f_{B_c} f_{D_s^*}, \quad a_2 \ \ is \ \ a \ \ parameter. \quad (12.c)$$

In MWTCM, using the Feynman rules in equation (5.a), equation (5.b) and the methods in Ref.[18], we can write down the amplitude of charged PGBs annihilation diagrams (see Fig.1.b):

$$M_b^{(p)} = i\varepsilon_{\mu\nu\alpha\beta}\eta^\mu k^\nu \epsilon^\alpha p^\beta f_{1(p)}^{anni} + \eta^\mu[\epsilon_\mu(m_{B_c}^2 - m_{D_s^*}^2) - (p+q)_\mu(\epsilon\cdot k)]f_{2(p)}^{anni} \quad (13)$$

with

$$f_{1(p)}^{anni} = -\zeta'[(\frac{e_s}{m_s}+\frac{e_c}{m_c})\frac{m_s-m_c}{m_{B_c}} + (\frac{e_b}{m_b}+\frac{e_c}{m_c})\frac{m_b-m_c}{m_{B_c}}]\frac{m_{B_c}m_{D_s^*}}{m_{B_c}^2 - m_{D_s^*}^2}, \quad (14.a)$$

$$f_{2(p)}^{anni} = \frac{1}{2}\zeta'[(\frac{e_s}{m_s}+\frac{e_c}{m_c})\frac{m_{D_s^*}}{m_{B_c}} + (\frac{e_b}{m_b}+\frac{e_c}{m_c})]\frac{m_{D_s^*}m_{B_c}}{m_{B_c}^2 - m_{D_s^*}^2}, \quad (14.b)$$

$$\zeta' = ea_2[\frac{2C_F}{m_{p_8^\pm}^2} + \frac{1}{12m_{p^\pm}^2}]\frac{V_{cb}V_{cs}^*}{F_Q^2} f_{B_c} f_{D_s^*}(m_{B_c}^2 + m_{D_s^*}^2). \quad (14.c)$$

The total annihilation amplitude (Fig.1.b) in the MWTCM is consequently the form of

$$\begin{aligned} M_b &= M_b^{(W)} + M_b^{(p)} \\ &= i\varepsilon_{\mu\nu\alpha\beta}\eta^\mu k^\nu \epsilon^\alpha p^\beta f_1^{anni} + \eta^\mu[\epsilon_\mu(m_{B_c}^2 - m_{D_s^*}^2) - (p+q)_\mu(\epsilon\cdot k)]f_2^{anni} \end{aligned} \tag{15}$$

with

$$f_1^{anni} = f_{1(W)}^{anni} + f_{1(p)}^{anni}, \tag{16.a}$$

$$f_2^{anni} = f_{2(W)}^{anni} + f_{2(p)}^{anni}. \tag{16.b}$$

3. Numerical results

We will use the following values for various quantities as input in our calculation.

(i). Decay constants for pseudoscalar B_c and vector meson D_s^*,

$$f_{D_s^*} = f_{D_s} = 344MeV$$

from the reports by three groups [19] and

$$f_{B_c} = 500MeV$$

from the results in Ref.[20].

(ii). Meson mass and the constituent quark mass,

$$M_{D_s^*} = 2.11GeV, \quad m_b = 4.7GeV, \quad m_c = 1.6GeV, \quad m_s = 0.51GeV$$

from the Particle Data Group [21], and

$$m_{B_c} = 6.27GeV$$

as estimated in Ref.[22]. We also use $m_{B_c} \approx m_b + m_c$, $m_{D_s^*} \approx m_s + m_c$ in our calculation.

(iii). The parameter a_2 appearing in nonleptonic B decays was recently extracted from the CLEO data [23] on $B \to D^*\pi(\rho)$ and $B \to J/\Psi K^*$ by H. Y. Cheng *et al.* [18]. Here, we take

$$a_2 = \frac{1}{2}(c_- - c_+) = 0.21.$$

(iv). For CKM elements [21], we use

$$V_{cb} = 0.04, \quad |V_{ts}| = V_{cb}, \quad |V_{cs}| = 0.9745, \quad V_{tb} = 0.9991.$$

(v). The QCD coupling constant $\alpha_s(\mu)$ at any renormalization scale can be calculated from $\alpha_s(m_Z) = 0.117$ via

$$\alpha_s(\mu) = \frac{\alpha_s(m_Z)}{1 - (11 - \frac{2}{3}n_f)\frac{\alpha_s(m_Z)}{2\pi}\ln(\frac{m_Z}{\mu})},$$

and we obtain

$$\alpha(m_b) = 0.203, \quad \alpha_s(m_W) = 0.119.$$

(vi). For the masses of $m_{p^\pm}$ and $m_{p_8^\pm}$ in MWTCM, Ref.[12] has presented a constraint on them, here we take

$$m_{p^\pm} = (100 \sim 250)GeV,$$

$$m_{p_8^\pm} = (300 \sim 600)GeV.$$

(vii). The decay constant F_Q satisfies the following constraint [12]:

$$F_\pi = \sqrt{F_\psi^2 + 3F_Q^2 + N_L F_L^2} = 246GeV.$$

It is found in Ref.[12] that $F_Q = F_L = 20 \sim 40GeV$. We will take

$$F_Q = 40GeV$$

in our calculation.

We give the long and short distance contributions to the form factors f_1 and f_2 in the SM and MWTCM in Table 1, so do the decay width in Table 2 using the amplitude formula,

$$\Gamma(B_c \to D_s^*\gamma) = \frac{(m_{B_c}^2 - m_{D_s^*}^2)^3}{32\pi m_{B_c}^3}(f_1^2 + 4f_2^2).$$

The lifetime of B_c was given in Ref.[24]. In this paper we use

$$\tau_{B_c} = (0.4ps \sim 1.35ps)$$

to estimate the branching ratio $BR(B_c \to D_s^*\gamma)$ which is a function of τ_{B_c}. The results are given in Table 3.

4. Discussion

We have studied two kinds of contributions to the process $B_c \to D_s^*\gamma$. For the short-distance one (as illustrated in Fig.1.a) induced by electromagnetic penguin, the momentum square of the hard scattering being exchanged by gluon is $3.6GeV^2$, which is large

enough for PQCD analyzing. The hard scattering process can not be included conveniently in the soft hadronic process described by the wave function of the final bound state. That is one important reason why we can not apply the commonly used spectator model [25] to the two body B_c decays. There is no phase-space for the propagators appearing in Fig.1.a to go on-shell, so the imaginary part of M_a is absent, unlike the situation in Ref.[6]. Another competitive mechanism is the weak annihilation. In SM, we find that it is more important than the former one. This situation different from that of the radiative weak $B^{\pm}$ decays which is overwhelmingly dominated by electromagnetic penguin. The results stem from two reasons: one is that the compact size of B_c meson enhances the importance of annihilation decays; the other comes from the Cabibbo allowance. In $B_c \to D_s^* \gamma$ process, the CKM amplitude of weak annihilation is $|V_{cb}V_{cs}^*|$, but in $B_{\pm} \to K^{\pm}\gamma$ process the CKM part is $|V_{ub}V_{us}^*|$, which is much smaller than $|V_{cb}V_{cs}|$.

In addition, we find that the contribution from PGBs in MWTCM to the short distance process $b \to s\gamma$ is too large due to the smallness of the decay constant F_Q in this model. In contrast, the contribution from PGBs through the weak annihilation process is negligibly small. In general, the modification from PGBs in MWTCM is too large to be consistent with the recent CLEO data on the branching ratio BR ($b \to s\gamma$).

In view of the above situation, we consider the TAMWTCM. The motivation of introducing topcolor to MWTCM is the following: in the original MWTCM, it is very difficult to generate the top quark mass as large as that measured in the Fermilab CDF and D0 experiments [26], even with " strong " ETC [27]. Thus, topcolor interactions for the third generation quarks seem to be required at an energy scale of about 1 TeV [28]. In the TAMWTCM, topcolor is still a walking theory to avoid the large FCNC [14]. As in other topcolor-assisted technicolor theories, the electroweak symmetry breaking is driven mainly by technicolor interactions which are strong near 1 TeV. The ETC interactions give contributions to all quark and lepton masses, while the large mass of the top quark is mainly generated by the topcolor interactions introduced to the third generation quarks. From Ref.[28], we can reasonably get the ETC-generated part of the top quark mass $m_t' = 66kGeV$ with $k \sim 1$ to 10^{-1}. To compare with the original MWTCM, we here take $m_t' = 35GeV$ as the input parameter in our calculation. (i.e., in the above calculations, $m_t = 174GeV$ is replaced by $m_t' = 35GeV$, the other calculations are the same as the original MWTCM), The corresponding results obtained in the framework of TAMWTCM

are also listed in the table 1, table 2 and table 3. From the results in these tables, we can see that the modifications from PGBs in topcolor assisted MWTCM to $B_c \to D_s^* \gamma$ are strongly suppressed relative to that in the original MWTCM. The branching ratio BR ($B_c \to D_s^* \gamma$) in TAMWTCM is therefore consistent with the recent CLEO constraint on the branching ratio BR ($b \to s\gamma$) for a certain range of the parameters.

In this paper, we neglected the contribution of the vector meson dominance VMD [29] due to the smallness of $J/\Psi(\Psi^{'}) - \gamma$ coupling.

Finally, we estimate the possibility of observing the interesting process of $B_c \to D_s^* \gamma$ at Tevatron and at the CERN Large Hadron Collider (LHC). The number of B_c at Tevatron and at LHC have estimated to be [30] 16000 (for 25 Pb^{-1} integrated luminosities with cuts of $P_T(B_c) > 10GeV$, $y(B_c) < 1$) and 2.1×10^8 (for 100 fb^{-1} integrated luminosities with cuts of $P_T(B_c) > 20GeV$, $y(B_c) < 2.5$), respectively. By comparing the above predicted number of B_c events with the branching ratio BR_{total}^{SM} ($B_c \to D_s^* \gamma$) as given in Table 3, one can understand that although this channel is unobservable at Tevatron, but more than one thousand events of interest will be produced at LHC, so it can be well studied at LHC in the future. Furthermore, it is easy to see that the branching ratio BR ($B_c \to D_s^* \gamma$) in the TAMWTCM is roughly one order higher than that in the SM. Therefore, if one find an clear surplus of B_c events in LHC experiments than that expected in the SM one may interpret it as a signal of new physics.

Acknowledgments

This work is supported by National Natural Science Foundation of China and the Natural Science Foundation of Henan Scientific Committee.

Reference

1. B. Grinstein *et al.*, Nucl. Phys. B 339, 269 (1990).

2. D. S. Du and Z. Wang, Phys. Rev. D 39, 1342 (1989); K. Cheng, T. C. Yuan, Phys. Lett. B 325, 481 (1994); Phys. Rev. D 48, 5049 (1994); G. Lu, *et al.*, Phy. lett. B 341, 391 (1995), Phys. Rev. D 51, 2201 (1995).

3. J. Tang, J. H. Liu and K. T. Chao, Phys. Rev. D 51, 3501 (1995); K. C. Bowler *et al.*, Phys. Rev. Lett. 72, 1398 (1994).

4. H. Leutwyler and M. Roos, Z. Phys. C 25, 91 (1984).

5. M. Neubert, Phys. Rep. 245, 1398 (1994).

6. A. Szczepaiak, *et al.*, Phys. Lett. B 243, 287 (1990); C. E. Carlson and J. MilRna, Phys. Lett. B 301, 237 (1993), Phys. Rev. D 49, 5908 (1994); *ibid* 51, 450 (95); H-n. Li and H. L. Yu, Phys. Rev. Lett 74, 4388 (1995).

7. Dongsheng Du, Gongru Lu, and Yadong Yang, BIHEP-TH-32 (submitted to Phys. Lett.B).

8. S. J. Brodsky and G. P. Lepage, Phys. Rev. D 22, 2157 (1980).

9. Cai-Dian Lü and Zhenjun Xiao, Phys. Rev. D 53, 2529 (1996).

10. S. Dimopoulos and L. Susskind, Nucl. Phys. B 155, 237 (1979); E. Eichten and K. Lane, Phys. Lett. B 90, 125 (1980).

11. T. Appelquist and G. Trintaphyllon, Phys. Lett. B 278, 345 (1992); R. Sundrum and S. Hsu, Nucl. Phys. B 391, 127 (1993); T. Appelquist and J. Terning, Phys. Lett. B 315, 139 (1993).

12. K. Lane and E. Eichten, Phys. Lett. B 222, 274 (1989); K. Lane and M. V. Ramana, Phys. Rev. D 44, 2678 (1991).

13. Chongxing Yue, Yuping Kuang and Gongru Lu, TUIMP-TH-95/72.

14. C. T. Hill, Phys. Lett. B 345, 483 (1995); K. Lane and E. Eichten, Phys. Lett. B 352, 382 (1995).

15. M. Battle *et al.*, CLEO Collaboration, Preprint, CLEO 93-13.

16. S. J. Brodsky and C. R. Ji, Phys. Rev. Lett 55, 2257 (1985).

17. Zhenjun Xiao, Lingde Wan, Jinmin Yang and Gongru Lu, Phys. Rev. D 49, 5949 (1994).

18. H. Y. Cheng, *et al.*, Phys. Rev. D 51, 1199 (1995).

19. A. Aoki, *et al.*, Prog. Theor. Phys. 89, 137 (1993); D. Acosta *et al.*, CLNS 93/1238; J. Z. Bai, *et al.*, BES Collaboration Phys. Rev. Lett. 74, 4599 (1995).

20. W. Buchmüiller and S-H. HTye, Phys. Rev. D 24, 132 (1994); A. Martin, Phys. Lett. B 93, 338 (1980); C. Quigg and J. L. Rosner, Phys. Lett. B 71, 153 (1977); E. Eichten *et al.*, Phys. Rev. D 17, 3090 (1978).

21. Particle Data Group, L. Montanet *et al.*, Phys. Rev. D 50, 1173 (1994).

22. W. Kwong and J. L. Rosner, Phys. Rev. D 44, 212 (1991).

23. CLEO Collaboration, M. S. Alam *et al.*; Phys. Rev. D 50, 43 (1994).

24. C. Quigg, FERMILAB-Conf-93/265-T; C. H. Chang and Y. Q. Chen, Phys. Rev. D 49, 3399 (1994); P. Colangelo, *et al.*, Z. Phys. C 57, 43 (1993).

25. M. Bauer *et al.*, Z. Phys. C 29, 637 (1985); B. Grinstein *et al.*, Phys. Rev. D 39, 799 (1987).

26. The CDF Collaboration, F.Abe et al., Phys. Rev. Lett. 74, 2626 (1995); The D0 Collaboration, S.Abachi et al., Phys. Rev. Lett. 74, 2697 (1995).

27. T. Appelquist, M. B. Einhorn, T. Takeuchi and L. C. R. Wijewardhana, Phys. Lett. B 220, 223 (1989); R. S. Chivukula, A. G. Cohen and K. Lane, Nucl. Phys. B 343, 554 (1990); A. Manohar and H. Georgi, Nucl. Phys. B 234, 189 (1984).

28. C. T. Hill, Phys. Lett. B 266, 419 (1991); S. P. Martin, Phys. Rev. D 45, 4283 (1992); D 46, 2197 (1992); Nucl. Phys. B 398, 359 (1993); M. Linder and D. Ross, Nucl. Phys. B 370, 30 (1992); C. T. Hill, D. Kennedy, T. Onogi and H. L. Yu, Phys. Rev. D 47, 2940 (1993); W. A. Bardeen, C. T. Hill and M. Lindner, Phys. Rev. D 41, 1649 (1990).

29. E. Golowich and S. Pakvasa, Phys. Rev. D 51, 1215 (1995); H. Y. Cheng, Phys. Rev. D 51, 6288 (1995).

30. K. Cheung, Phys. Rev. Lett 71, 3413 (1993).

Table 1: Form factors in the SM, MWTCM and TAMWTCM. f^{peng} and f^{anni} represent form factors for electromagnetic penguin and weak annihilation process, respectively.

f_i	SM	MWTCM	TAMWTCM
f_1^{peng}	-3.05×10^{-10}	$(0.50 \sim 1.13) \times 10^{-8}$	$(0.44 \sim 1.67) \times 10^{-9}$
f_2^{peng}	-1.57×10^{-10}	$(2.50 \sim 5.65) \times 10^{-9}$	$(2.22 \sim 8.38) \times 10^{-10}$
f_1^{anni}	7.10×10^{-10}	$(6.75 \sim 7.02) \times 10^{-10}$	$(6.75 \sim 7.02) \times 10^{-10}$
f_2^{anni}	-1.70×10^{-10}	$(-1.66 \sim -1.53) \times 10^{-10}$	$(-1.66 \sim -1.53) \times 10^{-10}$

Table 2: The decay rates in the SM, MWTCM and TAMWTCM. The Γ^{peng}, Γ^{anni} and Γ^{total} represent $\Gamma(B_c \to D_s^* \gamma)$ through penguin, annihilation, and penguin + annihilation diagrams, respectively.

$\Gamma(B_c \to D_s^* \gamma)$	SM	MWTCM	TAMWTCM
$\Gamma^{peng}(GeV)$	3.18×10^{-19}	$(0.86 \sim 4.36) \times 10^{-16}$	$(0.67 \sim 9.55) \times 10^{-18}$
$\Gamma^{anni}(GeV)$	1.06×10^{-18}	$(0.94 \sim 1.03) \times 10^{-18}$	$(0.94 \sim 1.03) \times 10^{-18}$
$\Gamma^{total}(GeV)$	9.92×10^{-19}	$(0.93 \sim 4.52) \times 10^{-16}$	$(0.23 \sim 1.26) \times 10^{-17}$

Table 3: The branching ratios ($B_c \to D_s^* \gamma$). The BR_{total}^{SM}, BR_{total}^{MWTCM}, $BR_{total}^{TAMWTCM}$ represent the branching ratio ($B_c \to D_s^* \gamma$) in the SM, MWTCM and TAMWTCM, respectively.

τ_{B_c}	0.4ps	1.0ps	1.35ps
BR_{total}^{SM}	6.03×10^{-7}	1.51×10^{-6}	2.04×10^{-6}
BR_{total}^{MWTCM}	$(0.57 \sim 2.75) \times 10^{-4}$	$(1.42 \sim 6.86) \times 10^{-4}$	$(1.91 \sim 9.26) \times 10^{-4}$
$BR_{total}^{TAMWTCM}$	$(1.37 \sim 7.66) \times 10^{-6}$	$(0.34 \sim 1.91) \times 10^{-5}$	$(0.46 \sim 2.58) \times 10^{-5}$

Figure caption

Fig.1: Fig.1.a shows the Feynman diagrams which contribute to the decay $B_c \to D_s^* \gamma$ through the short distance $b \to s\gamma$ mechanism. The blob represents the electromagnetic penguin operators contributing to $b \to s\gamma$. $x_2 p$ and $x_1 p$ are momenta of b and c quarks in the B_c meson, respectively. $y_2 q$ and $y_1 q$ are momenta of s and c quarks in the D_s^* meson, respectively. Fig.1.b represents the Feynman diagrams which contribute to the decay $B_c \to D_s^* \gamma$ through the weak annihilation.

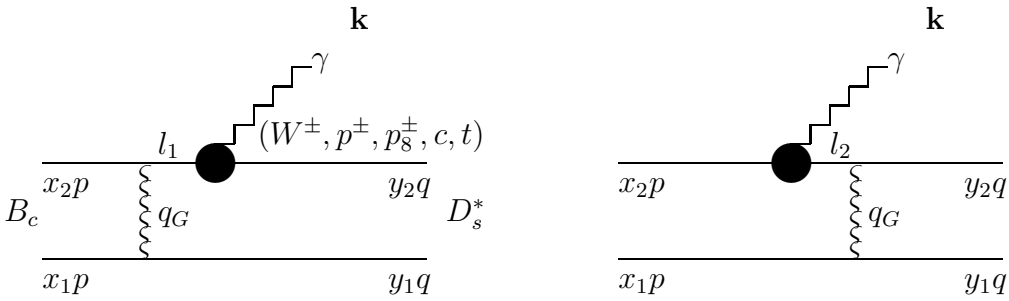
k
γ
$(W^{\pm}, p^{\pm}, p_8^{\pm}, c, t)$
l_1
x_2p
y_2q
B_c
q_G
D_s^*
x_1p
y_1q
k
γ
l_2
x_2p
y_2q
q_G
x_1p
y_1q

(a)

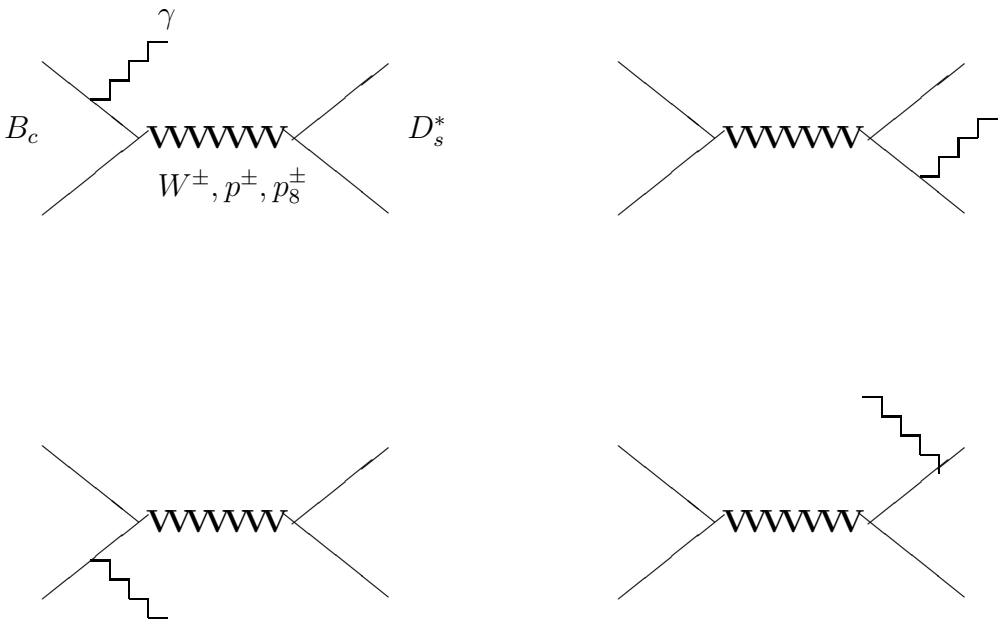
γ
B_c
D_s^*
$W^{\pm}, p^{\pm}, p_8^{\pm}$

(b)

Fig.1